Electronic Supplementary Information

Full Ring Closing in a Diarylethene Hexamer: Insights from Theory

Aurélie Perrier,[a] François Maurel,[a] Wesley R. Browne[b] and Denis Jacquemin[c,d,*]

a: Université Paris Diderot, Sorbonne Paris Cité, ITODYS, UMR CNRS 7086, 15 rue Jean Antoine de Baïf, 75205 Paris Cedex 13, France.
b: Center of System Chemistry, Stratingh Institute for Chemistry, Faculy of Mathematics and Natural Sciencres, University of Groningen, Nijenborgh 4, 9747AG Groningen, The Netherlands.
c: UMR CNRS 6230, Université de Nantes, CEISAM, 2 rue de la Houssinière, 44322 Nantes cedex 3, France. Fax: 33251125712; Tel: 33251125564; E-mail: Denis.Jacquemin@univ-nantes.fr
d: Institut Universitaire de France, 103, bd Saint-Michel, F-75005 Paris Cedex 05, France

A. Computational details

To perform our simulations, we have selected the latest version of the Gaussian program.[1] Our *ab initio* simulations consisted in geometry optimization and subsequent TD-DFT calculations of the different isomers using all possible closed/open combinations for the six photochromes. We have considered only the anti-parallel conformers here, as the parallel DA structures are known to be non-photochromic. The ground-state geometrical parameters have been determined at the PBE0/6-31G(d) level[2] via a force-minimization process. For the two fully symmetric structures, that belong to the C_6 point group, i.e. the systems that are fully closed and fully open, the vibrational spectra (both infrared and Raman) have been determined analytically at the same level of theory and it has been checked that these structures correspond to true minima of the potential energy surface. The spectra represented in section D use a scaling factor of 0.98 and have been obtained using convoluting Lorentzian presenting a FWHM of 2cm^{-}1 (IR) and 6cm^{-1}. For other symmetry lacking isomers, such determination could not be achieved due to the huge computational costs of analytic second-derivatives. The first thirty low-lying (isomers of **I**) excited-states have been determined within the vertical TD-DFT approximation using the CAM-B3LYP/6-31G(d) level of approximation,[3] as this range-separated hybrid has been shown adequate for investigating multi-DA architectures.[4] For the records, the typical cpu time required for computing 30 states is 250 days. Test calculations allowing quantifying the effects related to the solvent and the size of the atomic basis set have been performed as well (see Section B below). The simulated UV/Vis spectra use a broadening Gaussian of 0.25 eV of FWHM whereas the contour threshold for the molecular orbitals (MO) was set to 0.02 a.u. (model molecules) or 0.01 a.u. (**I**).

B. Methodological benchmarks

Obviously, the hexamer, **I**, is too large to allow any theoretical tests [performing a single TD-DFT calculation is already a significant computational challenge]. Therefore, to perform benchmarks, we have used two closely related DA "monomers" for which experimental data in exactly the same conditions are available.[5] These two molecules, **M1** and **M2** are sketched in Scheme S1 below.

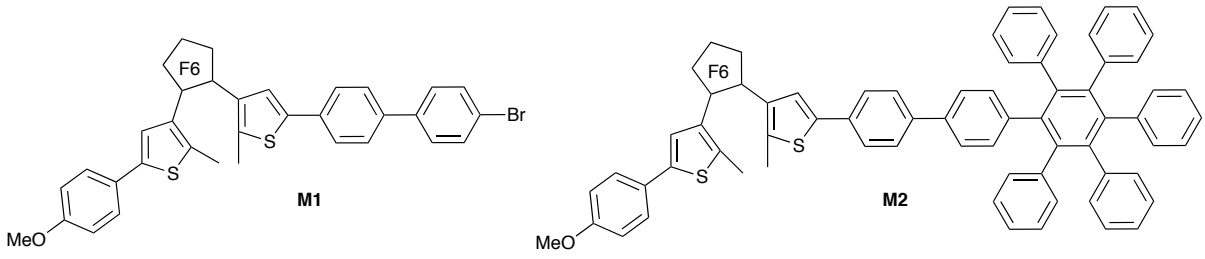

Scheme S1 Model monomers.

We have tested several computation protocols, using a known benchmark. More specifically, we performed computation with the 6-311G(d,p) and 6-311+G(2d,p) atomic basis sets that are known to yield fully converged geometries and transition energies for DA, respectively.[6] Our results can be found in Table S1. For the functionals, the choice of PBE0 for ground-state properties and CAM-B3LYP for excited properties is guided by

several previous theoretical investigations of multi-DA architectures,[4,7] and does not require further investigations.

Table S1 Relative Gibbs energies (kcal.mol^{-1}) of the closed and open forms of **M1** and **M2**, as well as λ_{max} (nm) computed with TD-DFT for the two isomers. Oscillator strengths are given between brackets. Different methods have been used to determine the geometrical (semi-empirical or DFT optimizations and free energy calculations) and spectral (ZINDO or TD-DFT simulations) properties of the two photochromes. When indicated, the PCM approach (toluene) is used to model solvent effects for both geometrical and spectral properties. Experimental values are from Ref 5. The results of the reference method are in blue, whereas the figures obtained with the methodology selected in the core of the Communication are in red.

	Geometry	Spectra	PCM	ΔG	λ_{max} Open	λ_{max} Closed
M1	PM6	CAM-B3LYP/6-31+G(d)	Y	+0.24	293 (0.11) 273 (1.51)	515 (0.48)
	PBE0/6-31G	CAM-B3LYP/6-31G		-0.20	321 (0.09) 289 (1.89)	535 (0.70)
			Y	+0.17	327 (0.12) 295 (1.96)	559 (0.81)
	PBE0/6-31G(d)	CAM-B3LYP/6-31G(d)		+10.1	297 (0.07) 289 (1.69)	543 (0.65)
			Y	+10.0	302 (0.09) 296 (1.80)	564 (0.75)
		CAM-B3LYP/6-31+G(d)			307(0.06) 296 (1.60)	556 (0.63)
			Y		312(0.10) 303 (1.70)	579 (0.73)
	PBE0/6-311G(d,p)	CAM-B3LYP/6-311+G(2d,p)		+9.63	309 (0.05) 297 (1.39)	562 (0.61)
			Y	+9.67	313 (0.06) 304 (1.58)	590 (0.73)
	Experiment	*Experiment*			*316*	*596*
M2	PM6	ZINDO	Y	+0.66	346 (1.01) 342 (0.24)	454 (0.78)
		CAM-B3LYP/6-31+G(d)	Y		294 (0.13) 276 (1.83)	516 (0.49)
	PBE0/6-31G	CAM-B3LYP/6-31G		+0.20	321 (0.09) 292 (2.25)	536 (0.79)
			Y	+2.21	327 (0.12) 298 (2.19)	559 (0.88)
	PBE0/6-31G(d)	CAM-B3LYP/6-31G(d)		+9.14	298 (0.06) 292 (2.15)	545 (0.73)
			Y	+9.21	302 (0.08) 297 (2.17)	566 (0.82)
		CAM-B3LYP/6-31+G(d)			308 (0.06) 299 (2.01)	558 (0.72)
			Y		313 (0.09) 304 (2.03)	581 (0.80)
	PBE0/6-311G(d,p)	CAM-B3LYP/6-311+G(2d,p)		+8.89	309 (0.07) 299 (1.98)	564 (0.70)
			Y	+8.84	314 (0.10) 304 (2.03)	587 (0.78)
	Experiment	*Experiment*			*324*	*602*

From Table S1, it is clear that both the semi-empirical ZINDO and PM6 methods as well as the tiny 6-31G atomic basis set should not be used: they provide incorrect relative energies for the two DA isomers, and for the former, very large errors (>100 nm/0.5e V) for the transition energies of the closed isomer. On the contrary, the 6-31G(d) basis set is sufficient to obtain accurate ΔG (errors smaller than 0.5 kcal.mol^{-1}), these relative energies being almost unaffected by solvent effects. In short, PBE0/6-31G(d) provides sufficiently accurate ground-state values for our purposes. As expected, the longest wavelength of maximal absorption are more signifiantly tuned by the selected approach. This is illustrated by the last column of Table S1. Using the 6-31G(d) basis set implies a shift of ca. 20 nm compared to the basis set limit. Likewise, performing gas-phase calculations also induces an additional shift of approximatively the same amplitude. Therefore the difference between the selected approach, CAM-B3LYP/6-31G(d), and the reference method, PCM-CAM-B3LYP/6-311+G(2d,p) reaches 47 nm and 42 nm for the closed forms of **M1** and **M2**, respectively. This corresponds to an overestimation of the transition energies of 0.18 eV and 0.16 eV, respectively. For the strongly allowed band in the UV domain of the open isomers, the errors are of the same order of magnitude in the energetic scale: 0.21 eV/0.17 eV for **M1**/**M2** (but of course smaller on the wavelength scale). The experimental λ_{max} of the closed **M1** (**M2**) is 596 (602) nm,[5] and the reference method is on the spot (less than 10 nm error for both photochromes). Consequently, the largest share of the experimental/theory discrepancy for **I** (see main text) can be attributed to the limitations of the size of the basis set and the lack of explicit solvent models rather than to inconsistencies in the CAM-B3LYP functional.

We have also evaluated the impact of dispersion effects on **M2**. To this end, we have optimized the closed isomer using both the B3LYP and B3LYP-D approaches and the 6-31G(d) basis set. Next, CAM-B3LYP/6-31G(d) calculations of the transition energies have been performed. The difference in λ_{max} determined on these two geometries was limited to 2 nm. This hints that the variations of geometry induced by dispersion effects have no significant impact on the spectroscopic signatures of the closed DA.

C. Orbital analysis for model compounds

The frontier molecular orbitals for **M1** and **M2** can be found in Figures S1 and S2, respectively. For the open isomer **M1(o)**, the two UV transitions at 289 and 297 nm, imply an orbital blend, but are dominated by H-1→L, H-1→L+1 and H→L, H→L+1 contributions, respectively. The occupied MO are located on one side of the DA bridge, whereas their virtual counterparts are centered on the DA core and the biphenyl side group. The LUMO of **M1(o)** presents a bonding character for to the to-be-formed CC single bond (the bond that is formed between the two reactive carbon atoms, see Scheme 2 and also see below for **M2**), which is typical of an efficient DA switch.[8,9] In **M1(c)**, the visible absorption calculated at 543 nm can be almost exclusively attributed to a HOMO to LUMO transition. As can be seen in Figure S1, these two orbitals are mainly localized on the DA core, with small contributions on the vicinal phenyls. These two MO present the shape that is typical of closed DA.[8,9] The LUMO+1 of **M1(c)** is delocalized on the full conjugated path but is located 1.3 eV above the LUMO and does not play a role in the optical properties.

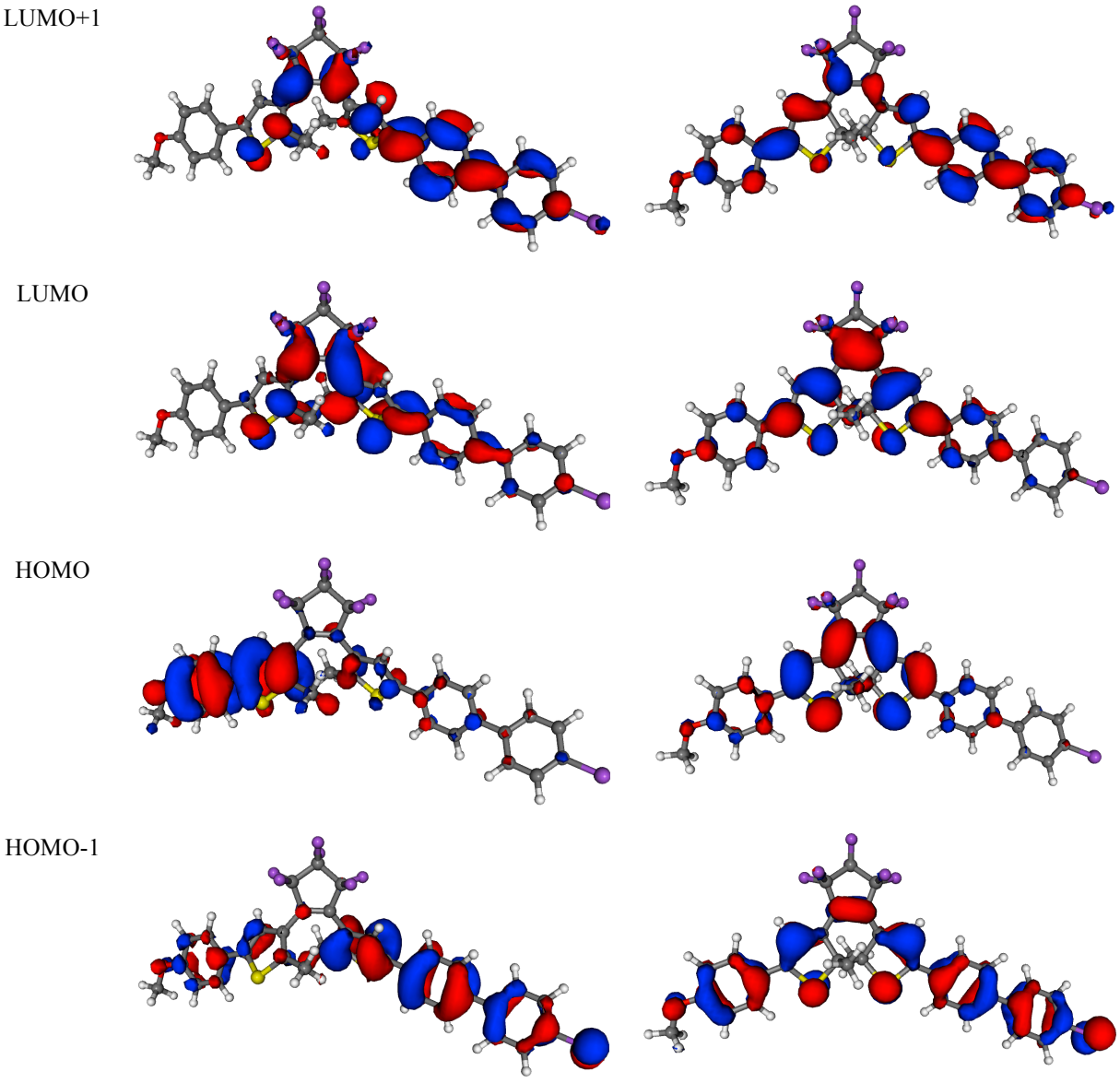

Figure S1 Front view of the frontier molecular orbitals of **M1** computed with the CAM-B3LYP/6-31G(d)//PBE0/6-31G(d) level for the open (left) and closed (right) isomers.

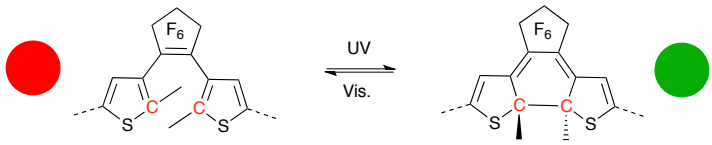

Scheme S2 Reactive carbon atoms in a DA switch (red). Adapted with permissions from *A. Perrier, F. Maurel, D. Jacquemin, Acc. Chem. Res.* ***45*** *(2012) 1173. Copyright 2012, American chemical Society*

For the **M2** structure that is a more adequate representation of the monomer of **I**, the two UV bands again correspond to electronic transitions from the two highest lying occupied MO towards the two lowest lying virtual MO (see Figure S2). While the LUMO+1 presents an antibonding character for the DA single CC bond and is mainly localized on the biphenyl systems, the LUMO presents the topology of unsubstituted DA,[8-10] In particular, the bonding character for the to-be-formed CC bond can explicitly be seen in Figure S3. Despite the limit of such Fukui-like model for complex photochromic situations, electronic transition to such orbital is an indication of photochromism for DA.[4,9,10] It is also noticeable that the topology of the LUMO of **M2(o)** is similar to the HOMO of **M2(c)**, which is also an hallmark of DA.[8] For **M2(c)**, the visible transition at 545 nm corresponds to an HOMO to LUMO transition. As can be seen in Figure S2, these two orbitals are localized on the DA core, like in **M1(c)**, the side hexaphenyl benzene system playing no role in the visible transition.

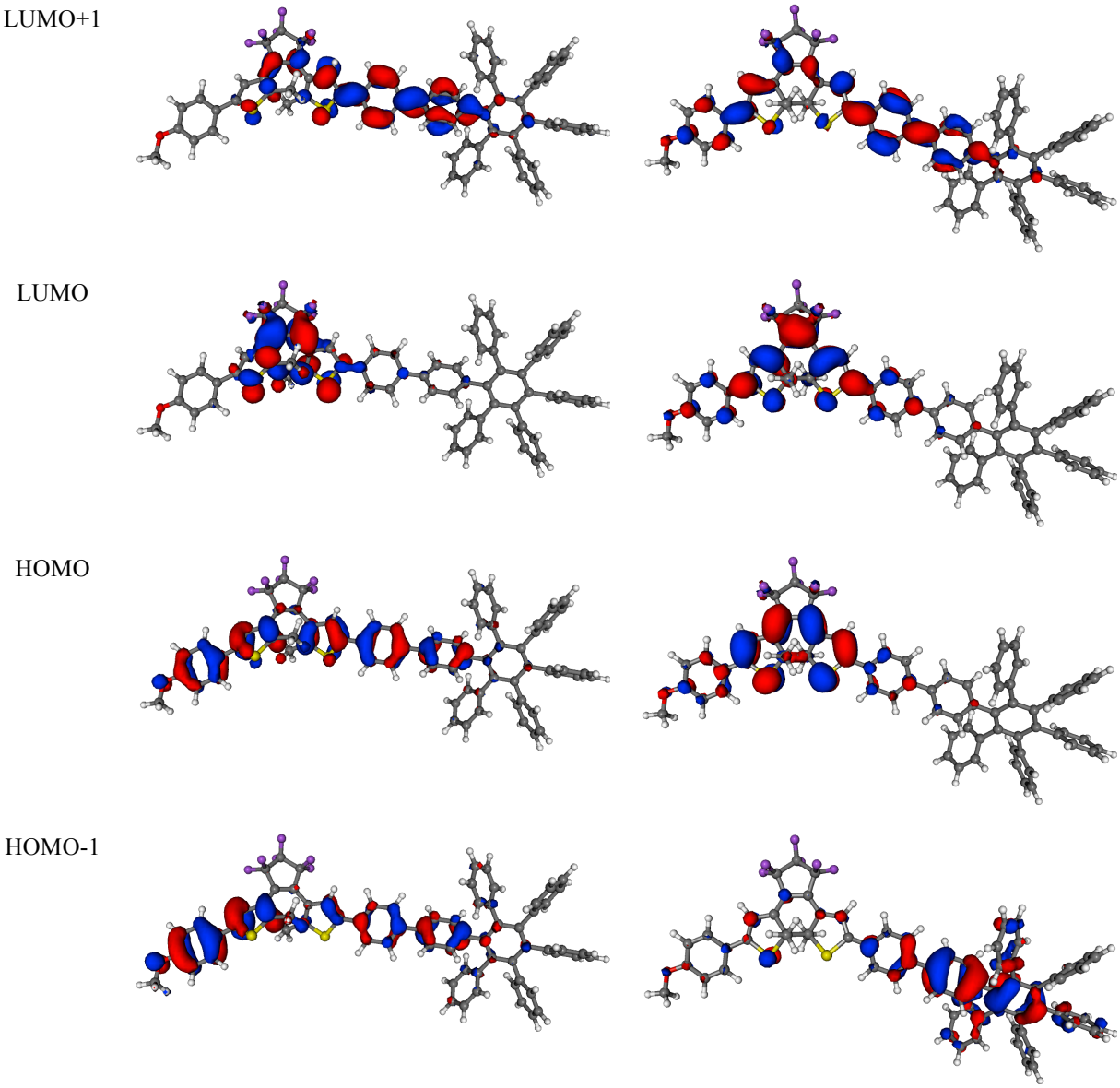

Figure S2 Front view of the frontier molecular orbitals of **M2** computed with the CAM-B3LYP/6-31G(d)//PBE0/6-31G(d) level for the open (left) and closed (right) isomers.

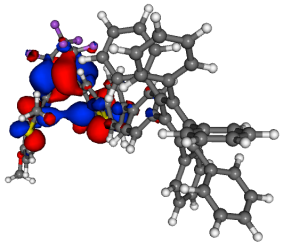

Figure S3 Side view of the LUMO of **M2(o)**. The bonding character of the π^* orbitals on the two reactive carbon atoms can be seen in blue. See caption of Figure S2 for more details.

D. Vibrational analysis of the fully open and fully closed isomers

The theoretical IR and Raman spectra computed for **I(6o)** and **I(6c)** are compared to the experimental data taken from Ref. 5 in Figure S4. For the IR spectra, the shape of both bands (double peak with almost the same intensity for **I(6o)**, more intense band with shoulder at larger energies for **I(6c)** is nicely reproduced by the calculation, as well as the relative positions, though the peak of **I(6c)** is computed ca. 15cm^{-1} above the experimental reference. For the Raman case, the evolution of the relative intensities of the two strongest bands upon cyclization of all DA is also restored by DFT, but the shape for the closed isomer is less satisfying.

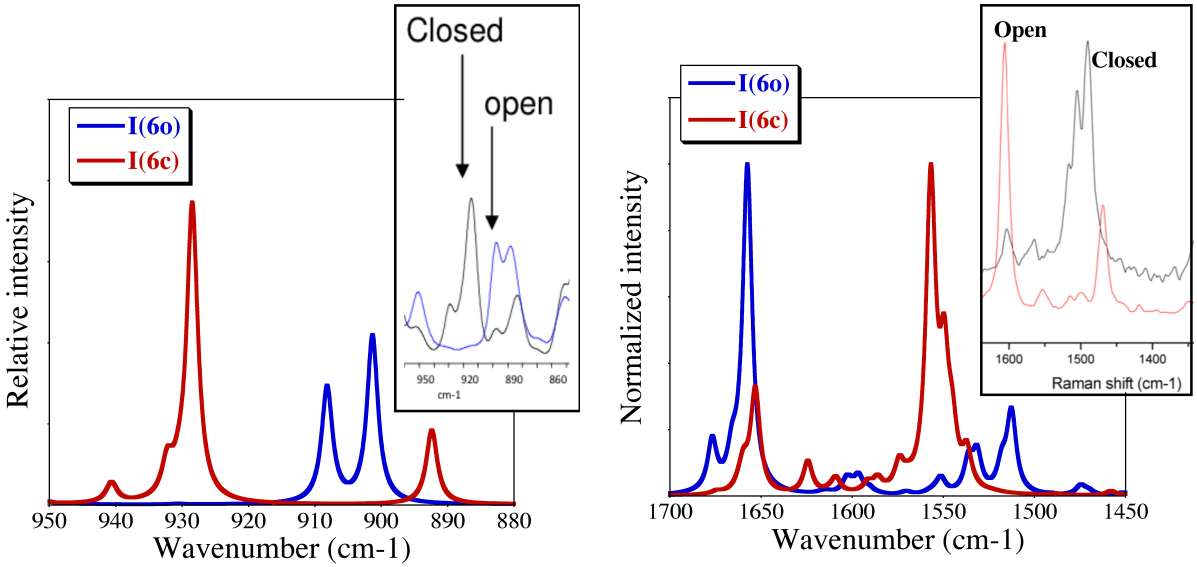

Figure S4 Computed IR (left) and Raman (right) spectra for fully open (blue curve) and fully closed (red curve) isomer. The experimental data are shown as inset and have been adapted with permission from Areephong, J. and Logtenberg, H. and Browne, W. R. and Feringa, B. L. *Org. Lett.* 2010, **12**, 2132–2135. Copyright 2010 American Chemical Society.

E. Relative energies and visible signatures for isomers of I

For the isomers of **I** presenting between two and four closed DA units, there are different possible spatial arrangements of the closed/open DA. They are represented in Figure S5. The **A** structures have vicinal closed DA whereas the **C** molecule present closed DA on opposite sides, **B** representing intermediate cases.

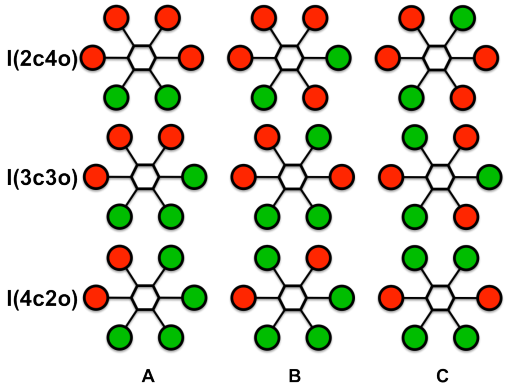

Figure S5 Simplified sketch of the possible isomers for doubly, triply and quadruply closed **I**. The red and green circles represent closed and open DA, respectively.

We have considered these different isomers, fully optimizing their geometry. The results are summarized in Table S2. As can be seen, all structures having the same number of closed/open DA units have almost the same energy (the difference being within the error bar of theory), indicating that in the experimental pot, there is probably a blend of different species. Likewise, the convoluted visible band presents the same position (±3 nm) and intensity (±0.02) irrespective of the **A**/**B**/**C** isomer. Therefore in the body of our communication we have systematically considered the most stable structures, rather than discussed negligible effects. Note that, in the raw TD-DFT results, the number of visible transition is strictly proportional to the number of closed DA, whereas the relative oscillator strengths of the individual (nearly degenerated) TD-DFT transitions are related to the pseudo-symmetry of the isomers, e.g. C_s-like for **I(2c4o)-A** but C_2-like for **I(2c4o)-C**, and are not to be interpreted independently.

Table S2 Relative total energies (kcal.mol^{-1}) of the **A**/**B**/**C** isomers, selecting the most stable system as reference, as well as the position of the visible band (in nm) computed before and after convolution with a broadening Gaussian. Oscillator strengths are given between brackets. All results obtained at the CAM-B3LYP/6-31G(d)//PBE0/6-31G(d) level of theory.

	Isomer	ΔE	Visible transitions (TD-DFT results)	Visible band (after convolution)
I(2c4o)	**A**	+0.20	552 (0.34) 544 (1.10)	546 (1.43)
	B	+0.12	550 (1.05) 546 (0.40)	549 (1.45)
	C	0.00	549 (1.42) 545 (0.01)	549 (1.43)
I(3c3o)	**A**	+0.04	552 (0.08) 549 (1.05) 541 (1.02)	546 (2.14)
	B	+0.06	552 (0.33) 549 (1.44) 543 (0.39)	548 (2.16)
	C	0.00	549 (1.07) 549 (1.07) 543 (0.02)	549 (2.15)
I(4c2o)	**A**	0.00	554 (0.04) 551 (0.52) 548 (1.43) 540 (0.37)	546 (2.86)
	B	+0.02	553 (0.19) 551 (0.88) 548 (1.13) 540 (0.37)	549 (2.86)
	C	+0.05	554 (0.32) 552 (0.41) 548 (2.09) 541 (0.05)	549 (2.87)

F. Selected MO for isomers of I

Below are reported some relevant MO for three isomers of **I**. In **I(6o)**, the LUMO+3, LUMO+4 and LUMO+5 (see Figure S6) present a photochromic shape (bonding character for the reactive carbon atoms), as the LUMO+2 reported in the main text and two other (not shown) virtual orbitals. In Figure S7, we give the two frontier orbitals of the singly closed isomer, **I(1c5o)**, and they are clearly centered on the closed DA. The visible band corresponds to a transition between these two orbitals, as expected. Finally, the HOMO of **I(6c)** is symmetric, and clearly localized on the DA rather than the central unit.

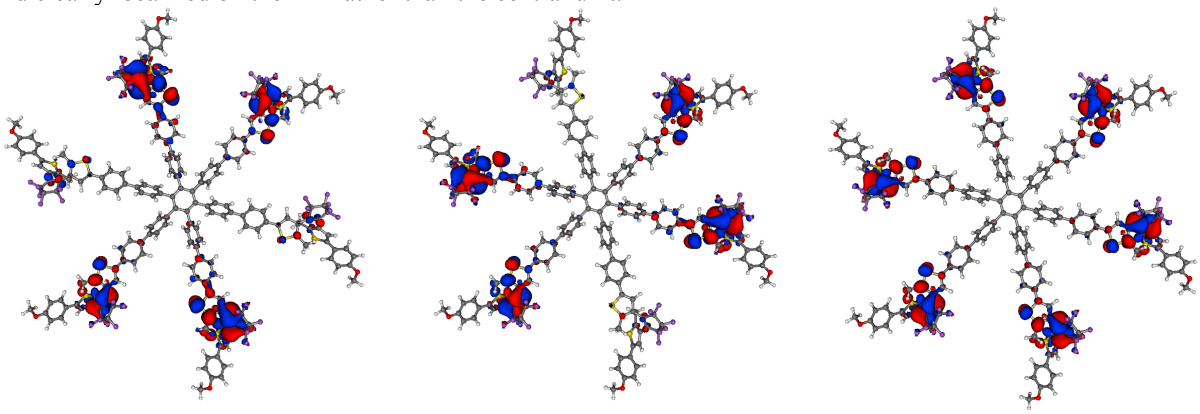

Figure S6 LUMO+3 (left), LUMO+4 (center) and LUMO+5 (right)of **I(6o)**.

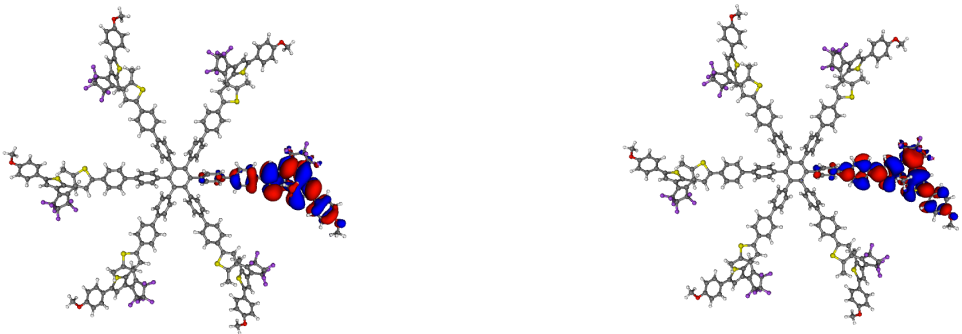

Figure S7 HOMO (left) and LUMO (right) of **I(1c5o)**. The two MO are centered on the single closed DA.

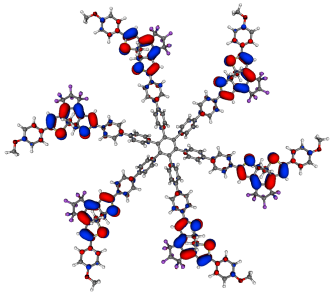

Figure S8 HOMO of **I(6c)**.

G. Alternative asymmetric hexamers

In Scheme S3, we propose six new hexamers: **A-1** that is similar to **I** but lacks of terminal OMe groups can be used as reference, **A-2** present three *normal* and three *inverse* DA, which are substituted with different electron donor/acceptors in **A-3**, **A-4** is constituted of three pairs of *normal(red)/inverse(blue)/semi-inverse(purple)* DA, and the same basic structures is used in both **A-5** and **A-6**, but conjugated bridging units are used.

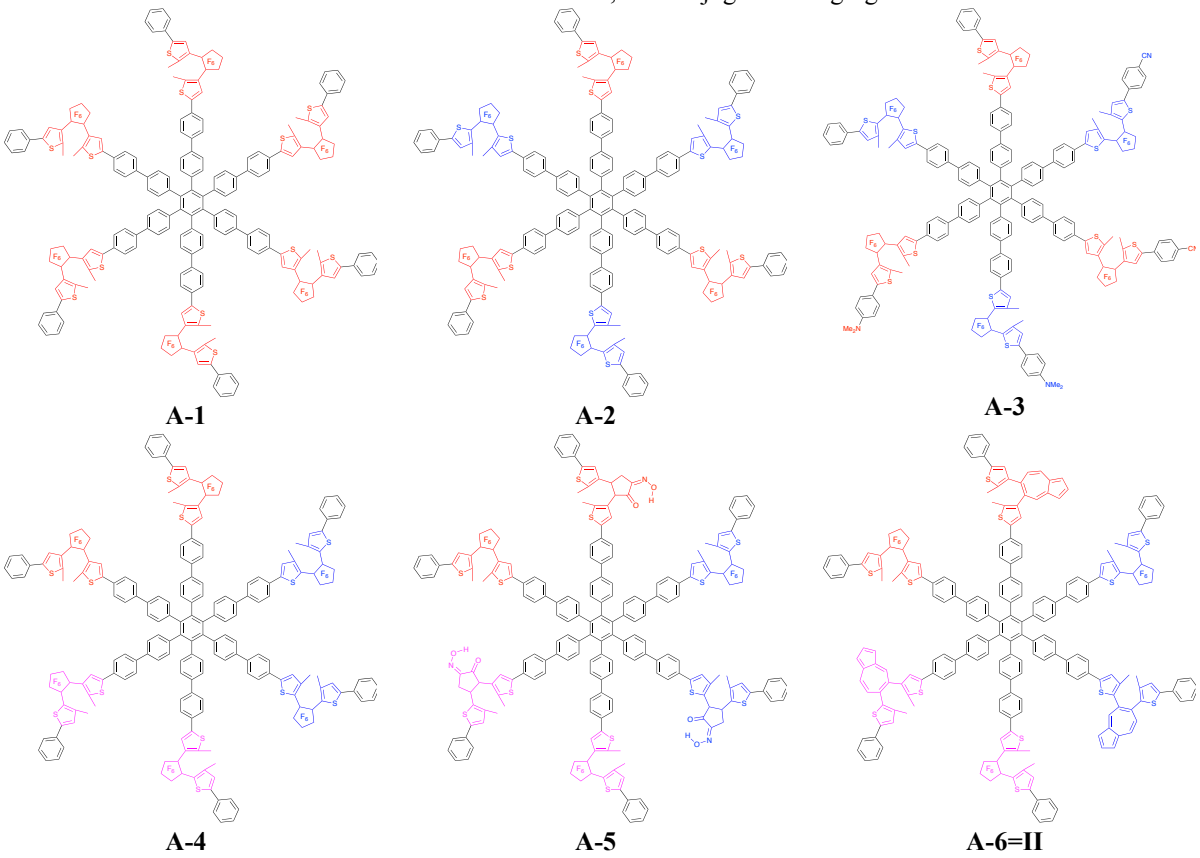

Scheme S3 Six (not yet synthesized) hexameric structures with various thiophene positions, terminal groups or bridging groups.

In Table S3 are listed the raw and convoluted TD-DFT (8 or more first excited states) results for these six structures in their fully closed forms. As can seen the use of inversed DA (like in **A-2**) yields the emergence of a new band closer to the UV limit, whereas conjugated bridges (**A-5** and **A-6=II**) induces bathochromic shifts of the visible absorption irrespective of the nature (normal/inverse/semi-inverse) of the selected DA. On the contrary, adding electron donors/acceptors (**A-3**) allows only for a small shift of the vertical transition energies and, consequently, after convolution, no additional bands are predicted (see **A-3** *versus* to **A-2** in Table S3).

Table S3 Computed visible transitions (λ > 350 nm) for the systems of Scheme S3 in their closed forms. All results obtained at the CAM-B3LYP/6-31G(d)//PBE0/6-31G(d) level of theory. See caption of Table S1 for more details.

	First visible transitions (First TD-DFT results for non-zero oscillator strength)	First visible bands (after convolution)
A-1	545 (1.90) 545 (1.90) 533 (0.07)	544 (3.86)
A-2	548 (0.93) 547 (0.94) 542 (0.05) 397 (0.10) 397 (0.09) 396 (0.06)	548 (1.92) 396 (0.25)
A-3	561 (0.92) 554 (0.79) 544 (0.43) 399 (0.07) 397 (0.08) 396 (0.08)	556 (2.08) 397 (0.23)
A-4	549 (0.31) 542 (1.03) 471 (0.26) 466 (0.75) 697 (0.05) 396 (0.12)	544 (1.33) 468 (1.01) 396 (0.17)
A-5	614 (0.46) 562 (0.41) 546 (0.65) 473 (0.14) 470 (0.46) 403 (0.01)	556 (1.07) 471 (0.61) 395 (0.11) 353 (1.09)
A-6	704 (0.32) 620 (0.23) 564 (0.06) 545 (0.66) 473 (0.51) 466 (0.14)	697 (0.34) 546 (0.71) 471 (0.66) 387 (1.56)

References

(1) Frisch, M. J. et al. Gaussian 09 Revision A.02 and C.01, 2009, Gaussian Inc. Wallingford CT.
(2) Adamo, C.; Barone, V. *J. Chem. Phys.* 1999, **110**, 6158–6170.
(3) Yanai, T.; Tew, D. P.; Handy, N. C. *Chem. Phys. Lett.* 2004, **393**, 51–56.
(4) Jacquemin, D.; Perpète, E. A.; Maurel, F.; Perrier, A. *J. Phys. Chem. C* 2010, **114**, 9489–9497.
(5) Areephong, J. and Logtenberg, H. and Browne, W. R. and Feringa, B. L. *Org. Lett.* 2010, **12**, 2132–2135.

(6) Jacquemin, D.; Perpète, E. A. *Chem. Phys. Lett.* 2006, **429**, 147–152.
(7) Perrier, A.; Maurel, F.; Jacquemin, D. *J. Phys. Chem. C* 2011, **115**, 9193–9203.
(8) Perrier, A.; Maurel, F.; Aubard, J. *J. PhotoChem. PhotoBiol. A: Chem* 2007, **189**, 167–176.
(9) Laurent, A. D.; André, J. M.; Perpète, E. A.; Jacquemin, D. J. *PhotoChem. PhotoBiol. A: Chem* 2007, **192**, 211–219.
(10) Perrier, A.; Maurel, F.; Jacquemin, D. *Acc. Chem. Res.* 2012, **45**, 1173–1182.